Published on 21 June 2018. Downloaded by INDIAN INSTITUTE OF TECHNOLOGY BOMBAY on 10/20/2020 4:50:29 PM.

Dalton Transactions

COMMUNICATION

View Article Online
View Journal | View Issue

Check for updates

Cite this: *Dalton Trans.*, 2018, **47**, 9980

Received 25th May 2018,
Accepted 20th June 2018

DOI: 10.1039/c8dt02145g

rsc.li/dalton

Deciphering the origin of invariance in magnetic anisotropy in $\{Fe^{II}S_4\}$ complexes: a theoretical perspective†

Arup Sarkar, Gunasekaran Velmurugan, Thayalan Rajeshkumar and Gopalan Rajaraman *

For q-bit applications based on coordination complexes, invariance in zero-field splitting parameters upon structural distortions is desired. Here, by employing *ab initio* calculations, we have probed the origin of such resistance observed in four coordinate $[Fe^{II}(C_3S_5)_2]^{2-}$ complexes. While unaltered *D* parameters are noted for a short range of structural distortions such as dihedral angle, if a wider range is chosen, larger variations are prominent in both *D* and *E*/*D* values.

Coordination complexes have longstanding use in the areas of molecular magnetism, magnetic refrigeration, magnetocaloric effect (MCE), molecular switches and also in the field of q-bits.[1] Among the Single Ion Magnets (SIMs), low coordinate complexes are of great interest as they offer attractive SIM characteristics.[2] On the other hand, spin-based q-bits have application in quantum information processing (QIP), quantum computing and other quantum simulation operations.[3] To generate quantum logic gate operations from electronic spin-based q-bits, at least two spin Eigen states are required in which spin transitions with superposition of states can be achieved over a long timescale.[4]

By fine-tuning the axial zero-field splitting parameter D and rhombic parameter E, one can obtain desirable spin Eigen states and for this reason zero-field splitting parameters have considerable importance in the area of spin based q-bits or multi q-bit systems.[4] These two parameters control the energy of separation between the M_S levels, which have been proposed to behave as quantum bits in nuclear spin-free high spin paramagnetic species. A multi-level M_S system could also serve as a multi-q-bit or a qudit system as has been proposed recently.[5] Particularly for the development of qudit systems proposed recently, the D parameter is relevant as this accounts for the splitting between the two q-bits.

For non-Kramers ions the D and E/D parameters are important as they dictate the quantum tunnelling of magnetization (QTM) between spin Eigen states (ΔM_S) differing by ±2 which in turn increases the relaxation for observing forbidden transitions in EPR spectroscopy.[4b,g]

While a number of experimental and theoretical studies focus on ways to fine-tune the D parameter, there are only a few reports on viable ways to tune the E parameter. Moreover, both D and E parameters are generally sensitive to small structural changes and therefore retaining the properties on surfaces upon adsorption is a challenging task.[6] In this regard, a report of three pseudo-tetrahedral $\{Fe^{II}S_4\}$ complexes – $[(18\text{-Crown-6})K]_2[Fe(C_3S_5)_2]$ (**1**), $(Ph_4P)_2[Fe(C_3S_5)_2]$ (**2**), and $(Bu_4N)_2[Fe(C_3S_5)_2]$ (**3**) assumes importance. The variation in the counter ion in complexes **1–3** leads to alteration in the dihedral angle (θ_d) between the two ligand planes from 72 to 90°; however the magnitudes of D and E are reported to be unaltered. The D and E/D parameters are estimated to be ~5.2 cm^{-1} and ~0.1, respectively (see Table 1), from HF-EPR and magnetic studies.[7] The invariance of D and E despite such a large variation in θ_d is remarkable; however, the electronic origin for such resistance has not been clearly understood. In this study, we aim to study complexes **1–3** and related models using high-level *ab initio* methods such as SA-CASSCF/NEVPT2 to underpin the reason behind the resistance observed.

Table 1 Comparison of experimental and theoretical (EPR), Mössbauer, ZFS and other structural parameters. Values given in parenthesis are for the molecules with counter ions

	1		**2**		**3**	
Complex	Calc.	Expt.	Calc.	Expt.	Calc.	Expt.
g_{min} (g_z)	2.00	2.00	2.00	2.00	2.00	2.00
g_{mid} (g_y)	2.07	2.02	2.06	2.07	2.05	2.04
g_{max} (g_x)	2.07	2.10	2.09	2.10	2.11	2.08
g_{iso}	2.05	2.04	2.05	2.07	2.05	2.11
D (cm^{-1})	6.12 (6.11)	5.21	6.07	5.35	6.01	5.61
E/D	0.02 (0.03)	0.11	0.11	0.11	0.24	0.10
θ_d	89.98°		81.38°		72.41°	
SHAPE (T_d)	2.065		2.073		3.515	
δ	0.546	0.680	0.539	0.663	0.542	0.677
ΔE_Q (mm s^{-1})	4.242	4.326	4.162	4.283	4.251	4.330

Department of Chemistry, Indian Institute of Technology Bombay, Powai, Mumbai, 400076, India. E-mail: rajaraman@chem.iitb.ac.in

†Electronic supplementary information (ESI) available. See DOI: 10.1039/c8dt02145g

This journal is © The Royal Society of Chemistry 2018

Published on 21 June 2018. Downloaded by INDIAN INSTITUTE OF TECHNOLOGY BOMBAY on 10/20/2020 4:50:29 PM.

The spin-Hamiltonian parameters have been calculated using the effective Hamiltonian approach (EHA) and this methodology has a proven record of accomplishment to reliably estimate such parameters (g, D and E) of transition metal complexes.[8] Here, we have employed the ORCA suite of programs for our calculations (see the ESI for elaborate discussion on computational details†).[9] In addition, we have also performed DFT calculations to evaluate the Mössbauer parameters (isomer shift δ and quadruple splitting ΔE_Q) to compare our values with the available experimental data (see Table 1).[10] Additionally quantum theory of atoms in molecules (QTAIM) analysis has been performed to probe the nature of bonding upon structural variation using the B3LYP/TZV setup employing the AIM2000 package.[11] We have performed the calculations on the X-ray crystal structures of complexes **1–3**. Calculations were performed in the presence and absence of the counter ion and this yielded a similar set of D values (see Table 1). This suggests that counter ions do not influence the D and E values. Also, we have optimized the geometry in the gas phase where significant structural deformations are detected leading to variations in the estimated D and E/D parameters (see ESI† for details). This suggests that the solid-state effects are important in dictating the structure and the associated experimentally observed parameters.

The coordination environment around the Fe^{II} centre in **1–3** (see Fig. 1) is an elongated tetrahedron with the SHAPE calculations revealing the deviation of 2.065, 2.073 and 3.515 for **1–3**, respectively, from an ideal tetrahedral geometry. This suggests that as we move from complex **1** to **3**, the distortion increases and complex **3** has the largest deviation from tetrahedral geometry (see Table 1 and S1†). The calculated D values in complexes **1–3** are very similar (6.12, 6.07 and 6.01 $cm^{-1}$for **1–3**, respectively) and all these values match well with the experiments. However, the calculations suggest that the E/D values increase from 0.02 to 0.11 and to 0.24 as we go from **1** to **3** (see Table 1). The close similarity among the computed D values in complexes **1–3** can easily be understood if we analyse the contributions to D utilizing symmetry arguments and also examine the QTAIM topological parameters (Table S2–S3 for QTAIM details in the ESI†). Complex **1** has a D_{2d} symmetry and the major anisotropy axes *i.e.*, D_{zz} and g_{zz} directions, were along the principal C_2 axis. Therefore, the ground state electronic configuration is $(d_{z^2})^2(d_{x^2-y^2})^1(d_{xy})^1(d_{xz})^1(d_{yz})^1$ where the d_{xz} and d_{yz} orbitals are very close in energy, with a computed gap of 35 cm^{-1} (see Fig. 1). Due to this high symmetry the major spin-allowed contribution to the positive D results from two transitions, which are $d_{z^2}(a_1) \rightarrow d_{yz}(e)$ and $d_{z^2}(a_1) \rightarrow d_{xz}(e)$. Besides, there is also a significant spin–flip transition taking place from $d_{x^2-y^2}(b_1) \rightarrow d_{xy}(b_2)$ orbitals that contributes to the total D value (4.9 cm^{-1}, 4.3 cm^{-1} and 3.5 cm^{-1} in complexes **1–3**, respectively). Note here that in terms of absolute magnitude, the contributions arising from spin–flip excitations are much larger than those from the spin-allowed excitations and hence these transitions were found to dictate the overall sign of the D values. The transitions mentioned here are correlated with the point group symmetry of the molecule and any alteration in the symmetry is thus likely to alter the sign/magnitude of D (see the ESI for details†).

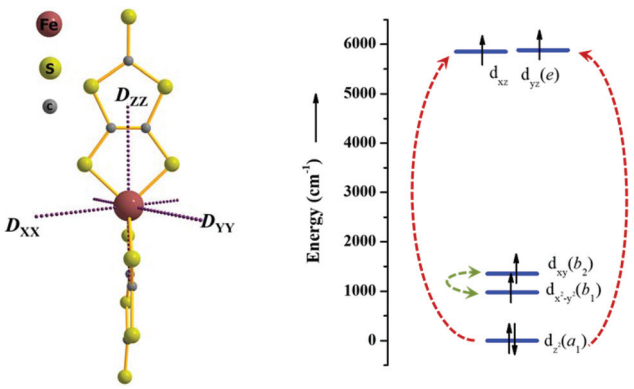

Fig. 1 X-ray structure of **1** along with the computed ZFS directions (right). Computed d-based orbital diagram showing prominent spin-allowed (dotted red) and spin-forbidden (dotted green) contributions to ZFS.

As we move from complexes **1–3**, the rhombicity clearly increases and this is attributed to the fact that the energy of the d_{xz} orbital decreases and the energy of the d_{yz} orbital increases. As a result, the d_{xz} orbital contribution to D increases while the contribution arising from the d_{yz} orbital decreases. As these two factors compete, the overall magnitude of D remains the same for all the three complexes, despite a drastic change in the dihedral angles. The energy difference (ΔE) between the d_{xz} and d_{yz} orbitals can be used to rationalise the variation in E/D values. These ΔE values are found to increase from 35 cm^{-1} to 1146 cm^{-1} and to 3681 cm^{-1}, as we move from complexes **1–3** (see Fig. S3 in the ESI†). This gap is correlated with the increase in the E/D value of 0.02, 0.11 and 0.24 for complexes **1–3**, respectively. This increase in the E/D value indicates a mixing of the ±1 states and consequently this induces spin tunnelling between the two states. Although the variation in the E/D value has not been experimentally observed, this may be due to the insensitive nature of the transitions to the variation in the E/D value as noted by the authors.[7] To ascertain confidence on the computed E/D values, we have simulated the available magnetic data using the computed parameters and these tend to reproduce the data very well (see Fig. **S4** in the ESI†).

To further probe the nature of the Fe–S bonding and its influence on the D and E parameters, we have performed QTAIM analysis. For complexes **1–3**, the electron density $\rho(r)$ at the BCP between Fe and S atoms (0.0642 au < $\rho(r)$ < 0.0663 au) and $\nabla^2_{\rho(r)}$ (0.0393 au < $\nabla^2_{\rho(r)}$ < 0.0426 au) is found to be small and positive. This indicates a closed shell character of the coordination bonds.[12] The $|V(r)|/G(r)$ < 1.0 to 1.28 found for these complexes suggests a mixed (largely ionic with a significant covalent component) character of these coordination bonds.[12b] The $\rho(r)$ values are found to increase, as we move from **1** to **3** and this corresponds to the increase in both the covalency and bond strength of Fe–S bonds.

It is important to note here that among complexes **1–3**, the largest deviation in the structural parameter is observed in the dihedral angle (θ_d), though smaller variations are also seen in

Published on 21 June 2018. Downloaded by INDIAN INSTITUTE OF TECHNOLOGY BOMBAY on 10/20/2020 4:50:29 PM.

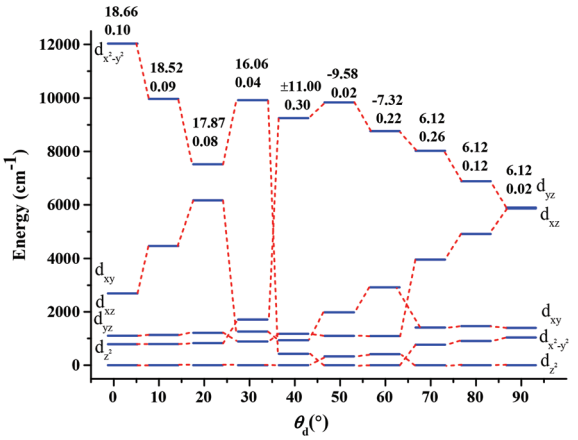

Fig. 2 Variation of d-orbital energies with respect to the dihedral angle. The values written above the diagrams are computed D and E/D values.

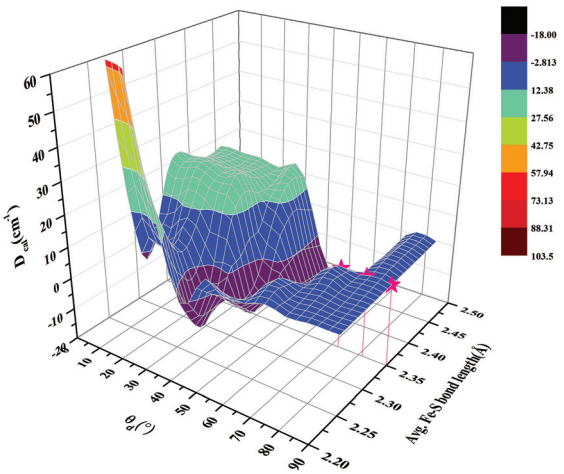

Fig. 3 Three-dimensional magneto-structural correlation developed by varying simultaneously θ_d and average Fe–S bond lengths. Here pink-stars represent complexes **1–3**.

other structural parameters. To fully comprehend the influence of the θ_d parameter on D and E, we have developed a correlation for the crystal structure of complex **1** by varying only the θ_d parameter. The computed results are shown in Fig. 2. The D and E parameters computed when the θ_d parameters are 80° and 69.9° are similar to the values obtained with the X-ray structures of **2** and **3**.

This affirms that the parameter D indeed does not alter upon variation in the θ_d parameter. Although the variation in the magnitude of D is not seen for θ_d in the range of 70–90°, D is found to be altered significantly for lower θ_d values. Particularly, at 64.7° of θ_d, the sign of D is found to switch to a negative value and here the E/D value is also very high. Here the positive contributions arising from spin–flip excitation disappear and this leads to a switch in the sign of D. At this point, the D_{ZZ} and g_{ZZ} orientations are also found to be switched and lie perpendicular to earlier axes. At lower dihedral angle, the geometry approaches towards square-planar and hence the direction of the anisotropy axis changes with the expected orbital ordering. At this point, the major contributions to the negative D correspond to the spin allowed transition from the $d_{x^2-y^2} \rightarrow d_{xy}$ orbital. As we move towards lower θ_d values, the sign of D is found to be switched. This happens when we reach the value of θ_d = 40° and at this point E/D is also found to be very large. Lowering θ_d further takes the structure closer to a square planar arrangement with a large positive D obtained at a θ_d value of 30.7° (D= + 16 cm^{-1}). Here, the beta electron resides in the d_{z^2} orbital leading to two positive spin-allowed transitions *i.e.*, $d_{z^2}(a_1) \rightarrow d_{yz}(e)$ and $d_{z^2}(a_1) \rightarrow d_{xz}(e)$ and hence a positive D value. This trend continues till a θ_d value of ~0°, with the D reaching up to ~20 cm^{-1} for a perfect square planar geometry (Fig. 3). The soft and weaker donor abilities of the S^{2-} ligand ensure a high-spin S = 2 ground state even for the square planar geometry.[13]

Next we turn to analyse the transverse anisotropy or E values, here up to a θ_d of 70°; the major contributions arise from the energy difference between the d_{xz} and d_{yz} orbitals as discussed above. Interestingly, below 70° of θ_d, the spin allowed contribution drastically decreases and a significant contribution from spin-forbidden transitions arises from $d_{z^2}(a_1) \rightarrow d_{xz}/d_{yz}(e)$ transitions (see equations in the ESI†).

In all the models with the θ_d variation, the Fe–S BCPs suggest that closed-shell interactions continue and the relation $|V(r)|/G(r) < 1.0$ also reveals partly covalent Fe–S interactions. As θ_d varies, the variation in $\rho(r)$ is also seen with $\rho(r)$ in the range of 0.0662–0.0645 yielding negative D values. The $\rho(r)$ values beyond this range are found to yield positive D values. Besides this, the Laplacian $\nabla^2_{\rho(r)}$ value is found to decrease with a decrease in the θ_d value, suggesting a greater charge concentration in the Fe–S region for the square planar arrangement and this also indicates that the bonds are becoming covalent as we reach the square planar geometry. A particularly relevant parameter in the QTAIM analysis is the local density energy $H(r)$, which tends to saturate for θ_d values of 0–30° and 65–90°; both ranges have a positive D. For θ_d in the range of 30–65°, significant variations are seen and these points correspond to a negative D value. Moreover, the ellipticity values (ε) computed at Fe–S BCP for models possessing θ_d values in the range of 0.15–0.05 are small and this correlates well with the observation of negative D values. For the same models, the valence shell charge concentration (VSCC) zone of the S atom is more diffused towards the Fe atom compared to that in other models and this indicates that there is a larger charge transfer from the S atom to the Fe atom.

Now that the role of the θ_d parameter on D and E values is established, we turn to investigate the effect of the Fe–S bond length on the anisotropy parameters. To understand how both θ_d and Fe–S bond lengths are correlated with each other, we have developed another magneto-structural correlation where both Fe–S bond lengths and θ_d parameters are simultaneously varied. This three-dimensional correlation developed is shown in Fig. 3. This graph shows two plateaus, one at higher θ_d values (blue plateau), which is also insensitive to variations in the Fe–S bond lengths and another at lower θ_d values (green

 This journal is © The Royal Society of Chemistry 2018

Published on 21 June 2018. Downloaded by INDIAN INSTITUTE OF TECHNOLOGY BOMBAY on 10/20/2020 4:50:29 PM.

plateau), which is sensitive to Fe–S bond lengths shorter than 2.35 Å. In general, we observed that the alteration in the bond length significantly influences the magnitude of the D parameter. Particularly, an increase in the Fe–S bond length is found to increase the $|D|$ values and the same is also true for very short Fe–S bond lengths. For very short Fe–S bond lengths of 2.25 Å, the magnitude of D tends to increase phenomenally at lower θ_d values reaching D= +100 cm^{-1} at square planar geometry (see the ESI for details†). At these geometries, the triplet states are found to be the ground state and they contribute significantly to the D value. A previous report suggests that the presence of hard donor ligand atoms at this bond length stabilises the triplet state leading to a spin-crossover phenomenon.[14]

For geometries possessing longer Fe–S bond lengths, as the Fe–S interactions are weakened, the metal d_{xz}/d_{yz} orbital energies are lowered and consequently the D value increases. Here, dominant contributions are found to arise only from the quintet states. This is also found to be supported by the QTAIM topological parameters such as $\rho(r)$, $\nabla^2_{\rho(r)}$ and $|V(r)|/G(r)$ and ε values at the BCP between Fe and the S atoms, which are found to decrease linearly with increasing Fe–S bond lengths. Clearly, a stronger dependence of D on Fe–S bond lengths and θ_d is visible in Fig. 3 where a variation of D from −18 to +103 cm^{-1} has been observed. A similar correlation for the E value suggests that the switching of the sign of D is always found to pass through a higher E (or E/D) value. Particularly, larger dihedral values are found to yield $E/D \sim 0.3$ more often than lower dihedral structures.

To this end, here we have employed *ab initio* calculations and bonding analysis to probe the variation of D and E/D values in complexes **1–3**, which are reported to resist changes in these parameters. While calculations reaffirm that the D values are unaltered for the reported structures, E values are found to vary. Additional calculations performed on model complexes suggest that the D value significantly varies if a wider window of θ_d parameters is considered; however, two clear platonic regions are noted. Particularly both the sign and magnitude of D are found to vary significantly if minor alterations in the Fe–S bond length are noted. As the bond length of the molecule is likely to be altered upon adsorption of the molecule on the surfaces[6,15]and this parameter is found to significantly influence the anisotropy here, it is important to target structures which possess a very strong metal–ligand bond strength for potential q-bit applications.

Conflicts of interest

There are no conflicts to declare.

Acknowledgements

GR would like to thank the SERB (EMR/2014/000247) for financial support. A. S. thanks the CSIR for a Senior Research Fellowship.

Notes and references

1 D. Gatteschi, R. Sessoli and J. Villain, *Molecular nanomagnets*, Oxford University Press on Demand, 2006.

2 (*a*) J. M. Zadrozny, D. J. Xiao, M. Atanasov, G. J. Long, F. Grandjean, F. Neese and J. R. Long, *Nat. Chem.*, 2013, **5**, 577–581; (*b*) J. M. Zadrozny, M. Atanasov, A. M. Bryan, C.-Y. Lin, B. D. Rekken, P. P. Power, F. Neese and J. R. Long, *Chem. Sci.*, 2013, **4**, 125–138; (*c*) S. Gómez-Coca, D. Aravena, R. Morales and E. Ruiz, *Coord. Chem. Rev.*, 2015, **289–290**, 379–392; (*d*) G. A. Craig and M. Murrie, *Chem. Soc. Rev.*, 2015, **44**, 2135–2147; (*e*) M. S. Fataftah, J. M. Zadrozny, D. M. Rogers and D. E. Freedman, *Inorg. Chem.*, 2014, **53**, 10716–10721; (*f*) D. E. Freedman, W. H. Harman, T. D. Harris, G. J. Long, C. J. Chang and J. R. Long, *J. Am. Chem. Soc.*, 2010, **132**, 1224–1225.

3 (*a*) S. Bertaina, S. Gambarelli, T. Mitra, B. Tsukerblat, A. Muller and B. Barbara, *Nature*, 2008, **453**, 203–206; (*b*) K. Bader, D. Dengler, S. Lenz, B. Endeward, S. D. Jiang, P. Neugebauer and J. van Slageren, *Nat. Commun.*, 2014, **5**, 5304; (*c*) J. M. Zadrozny, J. Niklas, O. G. Poluektov and D. E. Freedman, *ACS Cent. Sci.*, 2015, **1**, 488–492; (*d*) L. Tesi, E. Lucaccini, I. Cimatti, M. Perfetti, M. Mannini, M. Atzori, E. Morra, M. Chiesa, A. Caneschi, L. Sorace and R. Sessoli, *Chem. Sci.*, 2016, **7**, 2074–2083; (*e*) M. Affronte, F. Troiani, A. Ghirri, S. Carretta, P. Santini, V. Corradini, R. Schuecker, C. Muryn, G. Timco and R. E. Winpenny, *Dalton Trans.*, 2006, 2810–2817.

4 (*a*) M. N. Leuenberger and D. Loss, *Nature*, 2001, **410**, 789; (*b*) M. S. Fataftah, J. M. Zadrozny, S. C. Coste, M. J. Graham, D. M. Rogers and D. E. Freedman, *J. Am. Chem. Soc.*, 2016, **138**, 1344–1348; (*c*) M. S. Fataftah, S. C. Coste, B. Vlaisavljevich, J. M. Zadrozny and D. E. Freedman, *Chem. Sci.*, 2016, **7**, 6160–6166; (*d*) J. M. Zadrozny, J. Niklas, O. G. Poluektov and D. E. Freedman, *J. Am. Chem. Soc.*, 2014, **136**, 15841–15844; (*e*) F. Troiani and M. Affronte, *Chem. Soc. Rev.*, 2011, **40**, 3119–3129; (*f*) M. J. Graham, J. M. Zadrozny, M. Shiddiq, J. S. Anderson, M. S. Fataftah, S. Hill and D. E. Freedman, *J. Am. Chem. Soc.*, 2014, **136**, 7623–7626; (*g*) J. M. Zadrozny and D. E. Freedman, *Inorg. Chem.*, 2015, **54**, 12027–12031.

5 E. Moreno-Pineda, C. Godfrin, F. Balestro, W. Wernsdorfer and M. Ruben, *Chem. Soc. Rev.*, 2018, **47**, 501–513.

6 M. Mannini, F. Pineider, C. Danieli, F. Totti, L. Sorace, P. Sainctavit, M.-A. Arrio, E. Otero, L. Joly and J. C. Cezar, *Nature*, 2010, **468**, 417.

7 J. M. Zadrozny, S. M. Greer, S. Hill and D. E. Freedman, *Chem. Sci.*, 2016, **7**, 416–423.

8 (*a*) G. A. Craig, A. Sarkar, C. H. Woodall, M. A. Hay, K. E. R. Marriott, K. V. Kamenev, S. A. Moggach, E. K. Brechin, S. Parsons, G. Rajaraman and M. Murrie, *Chem. Sci.*, 2018, **9**, 1551–1559; (*b*) S. K. Singh and G. Rajaraman, *Nat. Commun.*, 2016, **7**, 10669; (*c*) M. Atanasov, D. Aravena, E. Suturina, E. Bill,

Published on 21 June 2018. Downloaded by INDIAN INSTITUTE OF TECHNOLOGY BOMBAY on 10/20/2020 4:50:29 PM.

D. Maganas and F. Neese, *Coord. Chem. Rev.*, 2015, **289–290**, 177–214; (*d*) R. Maurice, R. Bastardis, C. d. Graaf, N. Suaud, T. Mallah and N. Guihery, *J. Chem. Theory Comput.*, 2009, **5**, 2977–2984; (*e*) S. K. Singh, P. Badkur, T. Gupta and G. Rajaraman, *Chem. – Eur. J.*, 2014, **20**, 10305–10313.

9 F. Neese, *Wiley Interdiscip. Rev.: Comput. Mol. Sci.*, 2012, **2**, 73–78.

10 M. Römelt, S. Ye and F. Neese, *Inorg. Chem.*, 2008, **48**, 784–785.

11 (*a*) F. Biegler-König and J. Schönbohm, *J. Comput. Chem.*, 2002, **23**, 1489–1494; (*b*) T. Gupta, G. Velmurugan, T. Rajeshkumar and G. Rajaraman, *J. Chem. Sci.*, 2016, **128**, 1615–1630.

12 (*a*) E. Espinosa, I. Alkorta, J. Elguero and E. Molins, *J. Chem. Phys.*, 2002, **117**, 5529–5542; (*b*) S. Jenkins and I. Morrison, *Chem. Phys. Lett.*, 2000, **317**, 97–102.

13 J. Cirera, E. Ruiz and S. Alvarez, *Chem. – Eur. J.*, 2006, **12**, 3162–3167.

14 K. Ray, A. Begum, T. Weyhermüller, S. Piligkos, J. Van Slageren, F. Neese and K. Wieghardt, *J. Am. Chem. Soc.*, 2005, **127**, 4403–4415.

15 F. Totti, G. Rajaraman, M. Iannuzzi and R. Sessoli, *J. Phys. Chem. C*, 2013, **117**, 7186–7190.

 This journal is © The Royal Society of Chemistry 2018